ChemPubSoc Europe

DOI: 10.1002/cctc.201901315

CHEMCATCHEM Communications

Zeolite Surface Methoxy Groups as Key Intermediates in the Stepwise Conversion of Methane to Methanol

Michael Dyballa,*[a, b] Knut Thorshaug,[b] Dimitrios K. Pappas,[a] Elisa Borfecchia,[a, c] Karoline Kvande,[a] Silvia Bordiga,[a, c] Gloria Berlier,[c] Andrea Lazzarini,[a] Unni Olsbye,[a] Pablo Beato,[d] Stian Svelle,[a] and Bjørnar Arstad*[b]

This contribution clarifies the overoxidation-preventing key step in the methane-to-methanol (MTM) conversion over copper mordenite zeolites. We followed the methane-to-methanol conversion over copper mordenite zeolites by NMR spectroscopy supported by DRIFTS to show that surface methoxy groups (SMGs) located at zeolite Brønsted sites are the key intermediates. The SMGs with chemical shift of 59 ppm are identical to those formed on a copper-free reference zeolite after reaction with methanol and react with water, methanol, or carbon monoxide to yield methanol, dimethyl ether, and acetate. This reactivity corroborates the location of SMGs at Brønsted sites. We find no evidence for stable SMGs directly at copper sites and explain mechanistically why H-form mordenites outperform their Na-form analogues. This finding is of interest for any future process that tries to trap the intermediate methane oxidation product towards methanol.

Introduction

The direct oxidation of methane to methanol is a potential key technology for minimizing greenhouse gas emissions by converting stranded and flared methane into chemicals. The stepwise methane-to-methanol (MTM) conversion[1] based on Cu-exchanged zeolites has received great attention. The process consists of an initial activation/oxidation step (in O_2 or air), followed by a reaction step (with CH_4) and an extraction step (H_2O). Cu-exchanged mordenite (MOR) has shown a productivity per Cu of close to 0.5 mol_{MeOH}/mol_{Cu}.[2] Other frequently investigated materials are copper-exchanged zeolites with CHA,[3] MFI,[1a] MAZ,[4] and FER[5] topology. Even so, key points of the reaction still need clarification, such as (a) the configuration of the active site and (b) the nature and location of the initial oxidation intermediate that prevents overoxidation. For the active site (a), suggestions range from copper nanoparticles,[6] isolated mononuclear copper,[7] bridged dicopper sites,[1,2b,8] and bridged tricopper sites[9] Noteworthy, upon oxidation a reduction of copper from Cu^{II} to Cu^{I} occurs.[3,10]

In such a solvent-free reaction, over-oxidation of methane is detrimental and must be avoided by a stable intermediate (b), that can be subsequently extracted as methanol.[11] In this work, we attempt to reveal the nature of this key species. As this stable intermediate, Alayon et al.[10a] proposed a Cu^{I}–(OCH_3)–Cu^{II} group (along with the formation of Cu^{I}–(OH)–Cu^{II}) located at the (μ-oxo)dicopper site. These groups were commonly referred to as "methoxy-groups". Narsimhan et al.[12] claimed the identification of this species on Cu-MOR based on ^{13}C NMR spectroscopy, as they observed a peak at a chemical shift of 61 ppm. This shift is high compared to Surface Methoxy-Groups (SMG) located at Brønsted acidic sites.[13] Typical ^{13}C chemical shifts of such SMGs are 59 ppm on ZSM-5,[13b] between 61 ppm[13d] and 57 ppm[13e] on MOR and 56 ppm on zeolite Y.[13c] Adsorbed methanol species are typically reported between 50 and 54 ppm and the chemical shifts of dimethyl ether are usually around 61 ppm.[13a–c,e,f] It is known that these SMGs can be expelled as methanol by steam.[2,10b,14] It is also of particular relevance that SMGs are reactive in carbon monoxide carbonylation using Cu-zeolites, mordenite in particular.[12,13e] Recently, Sushkevich et al. found that the productivity of Cu,Na,H-MOR in methane oxidation was correlated to the amount of Brønsted sites in the material and these had a beneficial role in the intermediate stabilization.[15]

We prepared samples under flow conditions in a DRIFTS cell, for then to transfer the sample to a MAS rotor under Ar without exposure to air and water. The activation of the materials was conducted by heating up the samples in 10 ml/min O_2 to 773 K (for experimental details see Supporting Information (SI)). Samples were cooled in a controlled way and changes (in particular unwanted air and water exposure) was excluded by DRIFTS. Finally, the samples were transferred into

[a] Dr. M. Dyballa, D. K. Pappas, Dr. E. Borfecchia, K. Kvande, Prof. S. Bordiga, Dr. A. Lazzarini, Prof. U. Olsbye, Prof. S. Svelle
Department of Chemistry and Center for Materials Science and Nanotechnology (SMN)
University of Oslo
0315 Oslo (Norway)
E-mail: Michael.Dyballa@itc.uni-stuttgart.de
[b] Dr. M. Dyballa, Dr. K. Thorshaug, Dr. B. Arstad
SINTEF Industry
0373 Oslo (Norway)
E-mail: Bjornar.Arstad@sintef.no
[c] Dr. E. Borfecchia, Prof. S. Bordiga, Prof. G. Berlier
Department of Chemistry and INSTM Reference Center
University of Turin
10125 Turin (Italy)
[d] Dr. P. Beato
Haldor Topsøe A/S
Nymøllevej 55, 2800 Kgs. Lyngby (Denmark)

Supporting information for this article is available on the WWW under https://doi.org/10.1002/cctc.201901315

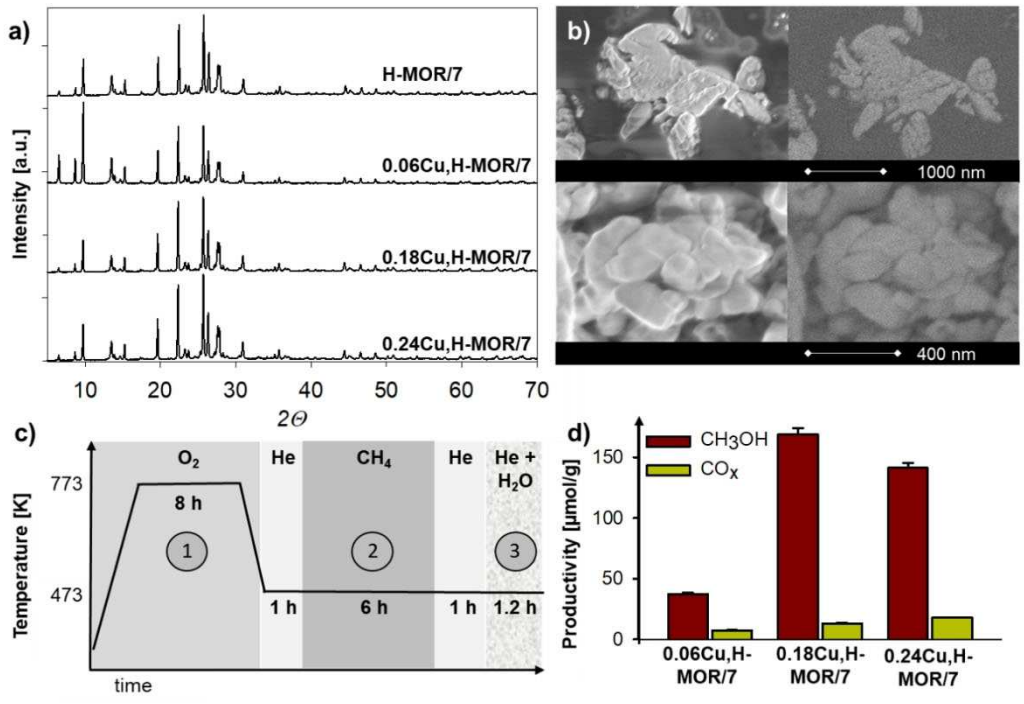

Figure 1. a) X-ray powder diffraction (XRD) patterns of parent and copper-exchanged material. b) Scanning electron microscopy (left) and high-angle backscattered electron detection (right) images of the highest copper loaded material 0.24Cu,H-MOR/7. c) The temperature program of the stepwise MTM conversion divided into oxidation (1), reaction (2), and extraction (3). d) Testing results for the *x*Cu,H-MOR/7 materials indicating an optimum performance for $x = 0.18$.

Table 1. Chemical characterization and testing data on parent and *x*Cu,H-MOR/7 materials.[2a]

Material	n_{Cu}/n_{Al} ratio[a]	Acid site density [mmol/g]	Cu [wt%]	BET[b] [m^2/g]	Selectivity S_{MeOH} [%]	Productivity [mol_{MeOH}/mol_{Cu}]	Productivity [$\mu mol_{MeOH}/g$]
H-MOR/7	–	2.00	–	520	–	–	–
0.06Cu,H-MOR/7	0.06	1.21	0.97	490	84	0.30	37
0.18Cu,H-MOR/7	0.18	1.08	2.33	440	93	0.47	169
0.24Cu,H-MOR/7	0.24	0.83	3.20	440	89	0.28	141

[a] Determined by EDX spectroscopy. [b] Specific surface area determined by BET analysis of N_2-adsorption measurements.

MAS NMR rotors under Argon and ex situ ^{1}H MAS NMR spectroscopy, ^{1}H-^{13}C cross-polarization (CP) MAS NMR spectroscopy, and ^{1}H-^{13}C heteronuclear correlation (HETCOR) spectroscopy were applied. In addition, a copper-free reference mordenite sample was investigated to obtain directly comparable spectra of regular SMGs at Brønsted sites.

The parent Mordenite zeolite, used in this study, was ion exchanged with copper acetate, resulting in *x*Cu,H-MOR zeolites with n_{Si}/n_{Al} ratio 7 and n_{Cu}/n_{Al} ratio *x* of 0 (parent, referred to as H-MOR/7), 0.06, 0.18, or 0.24.[2] X-ray powder diffraction (XRD) patterns of all materials are shown in Figure 1a and reflections belong to a pure MOR phase. No reflections indicating presence of bulk CuO are observed. Scanning electron microscopy (SEM, left) and high-angle backscattered electron detection (HA-BSED, right) of 0.24Cu,H-MOR/7 are shown in Figure 1b. The images reveal agglomerated zeolite crystals of 50 to 300 nm size and no bright spots, indicating the presence of CuO nanoparticles,[16] appear in the HA-BSED images. In line with *operando* X-ray absorption spectroscopy (XAS) studies, the active Cu site in these materials is atomically dispersed in mono-, di- and trinuclear configurations.[2b,14] Thus, the studied materials are of high crystallinity, phase pure, and the findings are not biased by CuO nanoparticles. Further standard characterization data are summarized in Table 1.

The three-step reaction cycle of the MTM conversion is shown in Figure 1c: (1) oxidation in O_2, (2) reaction with methane, and (3) extraction of methanol using water-saturated He-stream. Testing data shown in Figure 1d indicates a higher activity for the intermediate n_{Cu}/n_{Al} ratio, with a methanol productivity of 169 µmol/g (or 0.47 mol_{MeOH}/mol_{Cu}) and selectivity of up to 93%. Error bars indicate the inaccuracy resulting from elemental analysis and testing results.

Loadings with NH_3 were performed and quantified using ^{1}H MAS NMR after material dehydration in vacuum at 723 K (Figure S1 and S2 in the SI). Pure ^{1}H MAS NMR spectra of the samples before NH_3 loading show presence of Brønsted Si(OH)

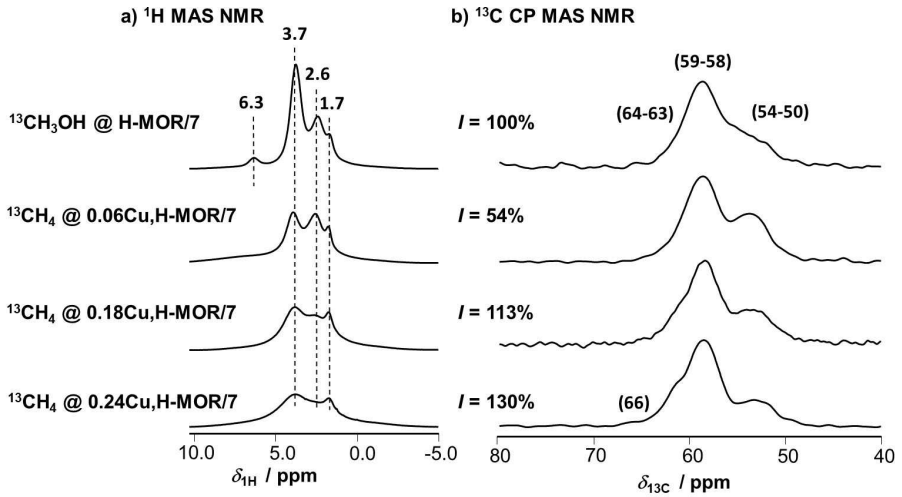

Figure 2. a) ^{1}H MAS NMR spectra of dehydrated samples after CH_3OH or CH_4 loading indicating Si(OH)Al groups and methoxy protons[13c] at 3.7 ppm, extra-framework Al(OH) groups at 2.6 ppm and external Si(OH) groups at 1.8 ppm. High copper loadings induce a significant broadening of ^{1}H peaks.[16] The methanol loaded parent material has traces of water at 6.3 ppm due to methanol dehydration.[19] b) Normalized ^{13}C CP MAS NMR spectra of total signal intensity *I* indicating presence of DME species (66; 64–63 ppm), SMGs (59–58 ppm), and methanol (54–50 ppm).[13b,c]

Al groups at 3.8 ppm, Al(OH) groups at 2.6 ppm, and Si(OH) groups at 1.8 ppm, respectively.[17] The acid site density (ASD) of these materials before reaction with methane (only Cu^{2+} present) was calculated by quantitative ^{1}H MAS NMR spectroscopy from the intensity of the NH_4^+-ion at 6.5 ppm. It ranges from 2.0 mmol/g to 0.83 mmol/g and thus decreases with rising n_{Cu}/n_{Al} ratio (see Table 1). These amounts are large compared to the quantity of formed Methanol (37 μmol/g to 176 μmol, see Table 1). Thus, the amount of acid sites is no limiting factor for the productivity in our H-form Mordenite system. It is however a reason for a lower productivity of comparable Na-form Mordenites.[2a] After ion exchange, traces of acid sites might be present that increase the methanol productivity.[15,18] A weak dealumination during activation at 723 K and above is indicated by peaks around 0 ppm in ^{27}Al MAS NMR spectra of hydrated samples (Figure S3 in the SI).[2a] Reduction of Cu^{2+} to Cu^{+} during the reaction, observed by *operando* XAS,[2b,10,14] also alters the acid site density (ASD) during the reaction. Thus, the ASD in Table 1 is not maintained during reaction but might increase.

As a definitive reference for SMGs at Brønsted sites, we loaded the copper-free parent H-MOR/7 with $^{13}CH_3OH$ to form SMGs at Brønsted sites (see Figure 2 top spectra: ^{1}H: 3.7 ppm, ^{13}C: 58–59 ppm).[13c] In ^{1}H-^{13}C CP MAS NMR spectra a high frequency shoulder between 60 and 64 ppm is attributed to end-on and side-on coordinated DME at Brønsted sites.[13e] The peaks in the range 50 to 54 ppm are due to methanol and minor amounts of SMGs at Si(OH).[13a,c,e] HETCOR spectra of methanol loaded parent H-MOR/7 are shown in Figure 3a. Cross-peaks indicate interaction between ^{1}H and ^{13}C nuclei in the two dimensions (F2/F1 ppm). An intense cross peak at 59/3.7 ppm belongs to methoxy protons interacting with their ^{13}C nuclei. The interaction of SMGs with Al(OH) groups of neighboring extra-framework aluminum is visible by a cross peak at 59/2.6 ppm, and is in line with the fairly high degree of dealumination of the parent zeolite.[2a] Furthermore, interaction

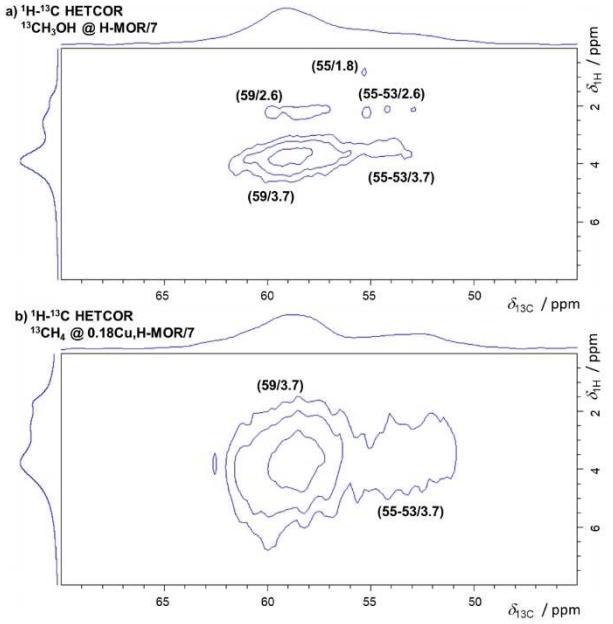

Figure 3. a) ^{1}H-^{13}C HETCOR spectra of H-MOR/7 loaded with methanol. b) ^{1}H-^{13}C HETCOR spectra of 0.18Cu,H-MOR/7 after reaction with methane. Cross peaks indicate interaction of SMG and methanol with Si(OH)Al, Al(OH), and Si(OH) groups, respectively. If copper is present, a symmetric broadening of peaks in F1-dimension is observed.

of free methanol with Si(OH) groups (55/1.8 ppm), Al(OH) groups (55–53/2.6 ppm), and Si(OH)Al groups (55–53/3.7 ppm) is observed.

With the base cases in place we continue with results from the MTM reaction over the Cu-exchanged MOR performed in the DRIFTS cell with subsequent NMR analyses. DRIFTS spectra of 0.24Cu,H-MOR collected during the activation can be found in the SI (Figures S4a–S4f). Briefly, while heating and maintain-

ing the sample at 773 K in synthetic air dehydration occurs, as testified by the disappearance of all the spectroscopic fingerprints of water accompanied by the growth of the bands associated to isolated Si(OH), Al(OH), Si(OH)Al, and eventually, Cu(OH) groups (S4a and S4b). After cooling down to 473 K and N_2 flush, four doses of $^{13}CH_4$ were reacted with the materials. This led to a reduction of the band intensity at 3648 cm^{-1} assigned to Al(OH) and probably Cu(OH) groups (S4c), while signals of $^{13}CO_2$ appeared and Cu^{+}—^{13}CO complexes form while the intensity of Brønsted and Si(OH) bands remained (Figure S4d). Subsequently, the samples were cooled (S4e and S4f) in dry N_2. Importantly, DRIFTS measurements confirmed that the samples do not change character by cooling from 473 K to room temperature hence the subsequent NMR experiments should be on samples representative for those at 473 K. The DRIFT protocol finally leads to $^{13}CH_4$ loaded materials *x*Cu,H-MOR/7 with x = 0.06, 0.18, and 0.24.

The ^{1}H-^{13}C CP MAS NMR spectra of $^{13}CH_4$ loaded materials are shown in Figure 2b). Main peaks belong to DME on Si(OH)Al at 64–60 ppm, SMGs around 59 ppm and both free methanol and SMGs at Si(OH) below 55 ppm.[13a,c, e] Remarkably, the chemical shifts and peak shapes of the investigated samples ($^{13}CH_3OH$ loaded parent, 3 × $^{13}CH_4$ loaded *x*Cu,H-MOR) are very similar, indicating that similar surface species have formed under the two different conditions. Also the overall peak shapes previously shown by Narsimhan et al.[12] agree well with ours and other literature examples,[13a,e] if their spectrum is corrected by 2 ppm (see the experimental part of the SI for referencing details). A shoulder at a chemical shift of 66 ppm appears on 0.24Cu,H-MOR/7 and belongs to Cu^{2+}-bound DME.[13a] On 0.06Cu,H-MOR a peak at 20 ppm is observed. It belongs to the CH_3-group of acetate, the carbonylation product formed from carbon monoxide (IR band at 2109 cm^{-1} in Figure S4d in the SI) and SMGs (see Figure S5 in the SI).[13a,e] ^{1}H-^{13}C HETCOR spectra of the Cu-loaded samples are found in Figure 3 and the SI (Figures S6a–S6b) and show cross peaks at (59/3.7 ppm) and at (55–53/3.7 ppm). Thus, the CH_4 activation leads to methoxy groups on the zeolite that are not directly bound to copper. These SMGs show an extraordinary stability: even after 7 months of storage in the MAS rotor at room temperature a ^{1}H-^{13}C CP MAS NMR spectrum of the 0.18Cu,H-MOR/7 sample was identical to the original spectrum acquired. We naturally associate this stability to the high selectivity towards methanol during extraction with steam. We conducted ^{1}H-^{13}C CP MAS NMR with different Hartmann-Hahn contact times to investigate eventual different dynamic states of SMGs such as in rigidly bound and free molecular species (see Figure S7 in the SI). The CP method relies on magnetization transfer from protons to carbons and differences in the dynamics between these atoms will result in variable intensities of the carbon peaks. A rigid species will typically show a quick build up to maximum intensity in contrast to a relatively more mobile species. By normalizing our spectra after such a set of experiments (Figure S7), it is clear that all spectra are similar. In addition, if strong paramagnetism close to the SMGs are present the CP method would likely result in variable build-up intensities for different species or precluded the application of the method at all due to very fast $T_1\rho$ relaxation. Thus (1) the flexibility/rigidity of SMG and "free" DME/methanol are similar and (2) the paramagnetic influence is weak.

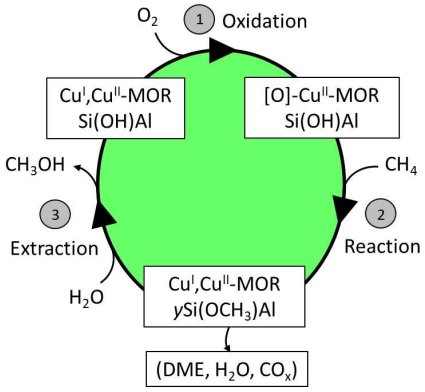

Scheme 1. Pathway of the stepwise MTM conversion according to the conditions stated in Figure 1c. Cu^{II} is present after oxidation (step 1), but gets reduced to Cu^{I} by methane (step 2). The reaction generates stable surface methoxy groups (SMGs) and as by-products traces of water, CO_x and DME. During extraction (step 3) the stoichiometric reaction of SMGs with water releases the methanol, whereby overoxidation to CO_x might occur.

The presented data and analyses enable us to suggest the MTM reaction pathway summarized in Scheme 1. The salient feature is the existence of SMGs on the zeolitic Brønsted acid sites after the CH_4 activation step. The formation of SMGs is accompanied by formation of H_2O, overoxidation products (CO, CO_2) and DME generated through methanol dehydration on acid sites. On H-form zeolites, the quantity of extraction products is usually small compared to the density of available Brønsted sites, in contrast to Na-form mordenites.[2a] This explains why H-form zeolites outperform their Na-form counterparts (where small amounts of Si(OH)Al are generated during ion exchange and when copper is reduced[20]) and why the methanol productivity correlates with the number of Brønsted acid sites.[15]

Conclusively, we identify two potential bottlenecks in the MTM reaction, namely (1) the absolute amount of active copper species, tunable by a properly adjusted stoichiometry,[2] and (2) the amount of Brønsted acid sites able to stabilize the SMG intermediate without overoxidation. For H-form mordenites, the quantity of Brønsted sites should usually be sufficient, as the degree of Cu exchange is limited. However, the key property of the sites hosting the SMGs must be the fast trapping of initial oxidation products. Thus overoxidation can be overcome by short diffusion pathways. This is usually realized by a good balance and proximity of Brønsted and copper sites. A high copper dispersion seems essential. Clearly, several intermediates exist during the MTM reaction.[10a] However, what we clearly observe is that methanol, dimethylether, and SMGs on Brønsted sites form and that these species are very stable under reaction conditions.

Summarizing, it can be stated that SMGs play a key role as intermediates for methanol and in preventing overoxidation of methane. Maximizing methanol output is reached by optimiz-

ing both n_{Si}/n_{Al} and n_{Cu}/n_{Al} ratio and alternately arranging copper and acid sites. With these new insights we can for the first time accurately explain why Na-form zeolites are outperformed by their H-form counterparts.

Supporting Information

Experimental explanations, DRIFTS spectra, additional ^{1}H, ^{13}C, ^{1}H-^{13}C HETCOR, and ^{27}Al MAS NMR measurements.

Acknowledgements

The authors acknowledge the iCSI (industrial Catalysis Science and Innovation) Centre for Research-based Innovation, which receives financial support from the Research Council of Norway under contract no. 237922. There are no conflicts to declare.

Conflict of Interest

The authors declare no conflict of interest.

Keywords: Copper Mordenite · Methane Oxidation · Methanol · Solid State NMR · Surface Methoxy Species

[1] a) M. H. Groothaert, P. J. Smeets, B. F. Sels, P. A. Jacobs, R. A. Schoonheydt, *J. Am. Chem. Soc.* **2005**, *127*, 1394–1395; b) P. J. Smeets, R. G. Hadt, J. S. Woertink, P. Vanelderen, R. A. Schoonheydt, B. F. Sels, E. I. Solomon, *J. Am. Chem. Soc.* **2010**, *132*, 14736–14738.

[2] a) M. Dyballa, D. K. Pappas, K. Kvande, E. Borfecchia, B. Arstad, P. Beato, U. Olsbye, S. Svelle, *ACS Catal.* **2019**, *9*, 365–375; b) D. K. Pappas, A. Martini, M. Dyballa, K. Kvande, S. Teketel, K. A. Lomachenko, R. Baran, P. Glatzel, B. Arstad, G. Berlier, C. Lamberti, S. Bordiga, U. Olsbye, S. Svelle, P. Beato, E. Borfecchia, *J. Am. Chem. Soc.* **2018**, *140*, 15270–15278.

[3] D. K. Pappas, E. Borfecchia, M. Dyballa, I. A. Pankin, K. A. Lomachenko, A. Martini, M. Signorile, S. Teketel, B. Arstad, G. Berlier, C. Lamberti, S. Bordiga, U. Olsbye, K. P. Lillerud, S. Svelle, P. Beato, *J. Am. Chem. Soc.* **2017**, *139*, 14961–14975.

[4] a) M. B. Park, S. H. Ahn, A. Mansouri, M. Ranocchiari, J. A. van Bokhoven, *ChemCatChem* **2017**, *9*, 3705–3713; b) A. J. Knorpp, A. B. Pinar, M. A. Newton, V. L. Sushkevich, J. A. van Bokhoven, *ChemCatChem* **2018**, *10*, 5593–5596.

[5] D. K. Pappas, E. Borfecchia, M. Dyballa, K. A. Lomachenko, A. Martini, G. Berlier, B. Arstad, C. Lamberti, S. Bordiga, U. Olsbye, S. Svelle, P. Beato, *ChemCatChem* **2018**.

[6] a) P. Tomkins, A. Mansouri, S. E. Bozbag, F. Krumeich, M. B. Park, E. M. Alayon, M. Ranocchiari, J. A. van Bokhoven, *Angew. Chem. Int. Ed.* **2016**, *55*, 5467–5471; *Angew. Chem.* **2016**, *128*, 5557–5561; b) S. E. Bozbag, P. Sot, M. Nachtegaal, M. Ranocchiari, J. A. van Bokhoven, C. Mesters, *ACS Catal.* **2018**, *8*, 5721–5731.

[7] P. Vanelderen, J. Vancauwenbergh, M. L. Tsai, R. G. Hadt, E. I. Solomon, R. A. Schoonheydt, B. F. Sels, *ChemPhysChem* **2014**, *15*, 91–99.

[8] a) E. M. Alayon, M. Nachtegaal, A. Bodi, M. Ranocchiari, J. A. van Bokhoven, *Phys. Chem. Chem. Phys.* **2015**, *17*, 7681–7693; b) P. Vanelderen, B. E. Snyder, M. L. Tsai, R. G. Hadt, J. Vancauwenbergh, O. Coussens, R. A. Schoonheydt, B. F. Sels, E. I. Solomon, *J. Am. Chem. Soc.* **2015**, *137*, 6383–6392.

[9] S. Grundner, M. A. Markovits, G. Li, M. Tromp, E. A. Pidko, E. J. Hensen, A. Jentys, M. Sanchez-Sanchez, J. A. Lercher, *Nat. Commun.* **2015**, *6*, 7546.

[10] a) E. M. C. Alayon, M. Nachtegaal, A. Bodi, J. A. van Bokhoven, *ACS Catal.* **2014**, *4*, 16–22; b) E. Borfecchia, D. K. Pappas, M. Dyballa, K. A. Lomachenko, C. Negri, M. Signorile, G. Berlier, *Catal. Today* **2019**, *333*, 17–27.

[11] M. Ravi, M. Ranocchiari, J. A. van Bokhoven, *Angew. Chem. Int. Ed.* **2017**, *56*, 16464–16483; *Angew. Chem.* **2017**, *129*, 16684–16704.

[12] K. Narsimhan, V. K. Michaelis, G. Mathies, W. R. Gunther, R. G. Griffin, Y. Roman-Leshkov, *J. Am. Chem. Soc.* **2015**, *137*, 1825–1832.

[13] a) L. Zhou, S. Li, G. Qi, Y. Su, J. Li, A. Zheng, X. Yi, Q. Wang, F. Deng, *Solid State Nucl. Magn. Reson.* **2016**, *80*, 1–6; b) W. Wang, A. Buchholz, M. Seiler, M. Hunger, *J. Am. Chem. Soc.* **2003**, *125*, 15260–15267; c) Y. Jiang, W. Wang, V. R. Marthala, J. Huang, B. Sulikowski, M. Hunger, *J. Catal.* **2006**, *238*, 21–27; d) E. G. Derouane, J. P. Gilson, J. B. Nagy, *Zeolites* **1982**, *2*, 42–46; e) T. Blasco, M. Boronat, P. Concepcion, A. Corma, D. Law, J. A. Vidal-Moya, *Angew. Chem. Int. Ed.* **2007**, *46*, 3938–3941; *Angew. Chem.* **2007**, *119*, 4012–4015; f) M. W. Anderson, J. Klinowski, *J. Am. Chem. Soc.* **1990**, *112*, 10–16.

[14] K. A. Lomachenko, A. Martini, D. K. Pappas, C. Negri, M. Dyballa, G. Berlier, S. Bordiga, C. Lamberti, U. Olsbye, S. Svelle, P. Beato, E. Borfecchia, *Catal. Today* **2019**.

[15] V. L. Sushkevich, J. A. van Bokhoven, *Catal. Sci. Technol.* **2018**, *8*, 4141–4150.

[16] M. Dyballa, D. K. Pappas, E. Borfecchia, P. Beato, U. Olsbye, K. P. Lillerud, B. Arstad, S. Svelle, *Micropor. Mesopor. Mater.* **2018**, *265*, 112–122.

[17] M. Hunger, *Solid State Nucl. Magn. Reson.* **1996**, *6*, 1–29.

[18] M. Dyballa, U. Obenaus, M. Blum, W. Dai, *Catal. Sci. Technol.* **2018**, *8*, 4440–4449.

[19] M. Hunger, D. Freude, H. Pfeiffer, *J. Chem. Soc. Faraday Trans.* **1991**, *87*, 657–662.

[20] a) Y. Li, W. K. Hall, *J. Catal.* **1991**, *129*, 202–215; b) D. J. Parrillo, D. Dolenec, R. J. Gorte, R. W. McCabe, *J. Catal.* **1993**, *142*, 708–718.

Manuscript received: July 22, 2019
Revised manuscript received: August 22, 2019
Accepted manuscript online: August 22, 2019
Version of record online: September 25, 2019